The spatial and metabolic basis of colony size variation

Jeremy Chacón[1,2], Wolfram Möbius[3,4], William Harcombe[1,2]

[1] Department of Ecology, Evolution and Behavior, University of Minnesota, St. Paul, MN, USA
[2] BioTechnology Institute, University of Minnesota, St. Paul, MN, USA
[3] Living Systems Institute, University of Exeter, Exeter, UK
[4] College of Engineering, Mathematics and Physical Sciences, University of Exeter, Exeter, UK

Running Title – Location's effect on competition between colonies

Corresponding Author
William Harcombe
1479 Gortner Ave.
St. Paul, Minnesota, 55108
612-301-1164
612-625-5780 (fax)
harcombe@umn.edu

Conflicts of interest
The authors declare no conflicts of interest.

Subject Category
Microbial population and community ecology

Abstract

Spatial structure impacts microbial growth and interactions, with ecological and evolutionary consequences. It is therefore important to quantitatively understand how spatial proximity affects interactions in different environments. We test how proximity influences colony size when either *Escherichia coli* or *Salmonella enterica* are grown on different carbon sources. The importance of colony location changes with species and carbon source. Spatially-explicit, genome-scale metabolic modeling predicts colony size variation, supporting the hypothesis that metabolic mechanisms and diffusion are sufficient to explain the majority of observed variation. Geometrically, individual colony sizes are best predicted by Voronoi diagrams, which identify the territory that is closest to each colony. This means that relative colony growth is largely independent of the distance to colonies beyond those that set territory boundaries. Further, the effect of location increases when colonies take-up resource quickly relative to the diffusion of limiting resources. These analyses made it apparent that the importance of location was smaller than expected for experiments with colonies growing on sugars. The accumulation of toxic byproducts appears to limit the growth of large colonies and reduce variation in colony size. Our work provides an experimentally and theoretically grounded understanding of how location interacts with metabolism and diffusion to influence microbial interactions.

Introduction

Microbial interactions help determine ecosystem functions, from global nutrient cycling to human health(Cho & Blaser 2012; Arrigo 2005). Spatial structure mediates microbial interactions (Connell et al. 2014), however, the relationship between proximity and strength of interaction remains unclear (Nadell et al. 2016). Quantifying, and being able to predict, the effect of location on microbial interactions is critical for understanding processes from the community evolutionary-ecology of microbial ecosystems to emergent functions such as human health.

Spatial structure modulates the resource competition that shapes microbial communities (Mitri & Foster 2013, Foster & Bell 2012, Stacey et al 2016). The relative strength of competition influences community assembly (David et al. 2015) and stability (Shade et al. 2012), in addition to shaping the selection on microbial traits (Gerardin et al. 2016). Spatial structure alters the scope of competition (Mitri & Foster 2013). In agitated liquid environments all cells tend to have equal access to resources and interactions are global. In contrast, in structured environments, cells interact more strongly with neighbors than with distant individuals. This localizing effect of spatial structure has been repeatedly shown to influence the outcomes of microbial evo-ecological experiments (Gerardin et al. 2016; Mitri et al. 2015; Harcombe et al. 2014; Allen et al. 2013; Allison 2005; Kim et al. 2008; Hansen et al. 2007; Kerr et al. 2002; Greig & Travisano 2008; Dechesne et al. 2008; Chao & Levin 1981; Penn et al. 2012; Gralka et al. 2016).

66 The specific location of bacteria in spatially-structured environments matters. Within a biofilm
67 or colony, bacteria at the edge have smaller local density and grow faster than those in the
68 center (Persat et al. 2015; Gandhi et al. 2016; Nadell et al. 2016; Pirt 1967), which can segregate
69 competing genotypes (Korolev et al. 2012; Mitri et al. 2015; Hallatschek & Nelson 2010;
70 Hallatschek et al. 2007; Momeni et al. 2014). Between-colony interactions are also influenced
71 by colonies' locations. A competing colony's effect is magnified if it is located between a focal
72 colony and a nutrient source(Harcombe et al. 2014). Further, the coexistence of competing
73 genotypes can be highly sensitive to the distance between colonies (Gerardin et al. 2016; Kim et
74 al. 2008). Finally, hints of the importance of location are also being detected in complex natural
75 ecosystems, such as in the microbiome. For example, changes in the spacing between
76 *Aggregatibacter actinomycetemcomitans* and *Streptococcus gordonii* determine virulence in
77 oral abscesses(Stacy et al. 2014).
78
79 While it is known that location matters, we lack a rigorous framework for understanding and
80 predicting the impact of location on interactions. Interaction strength can be a function of
81 distance(Kim et al. 2008), but by what distance-based measurement? The distance to the
82 closest competitor, a function of all competitor distances, or a measurement of how
83 competitors divide the available territory? Ecologists often use distance metrics to explain
84 variance in plant growth(Tome & Burkhart 1989), and a linearly-weighted distance model
85 captured a decline in bacterial colony size due to crowding (Guillier et al. 2006). In contrast,
86 Voronoi diagrams, which measure the territory that is closer to a focal colony than any other
87 colonies(Okabe et al. 2000), have been used to investigate pattern formation as bacteria cover

a surface(Lloyd & Allen 2015). To date there has not been a rigorous test of the ability of different geometric models to explain variance in colony size.

In addition to this geometric description, the question arises what minimal biophysical model can predict the location-based effects on colony growth in variable environments. Microbes typically interact through the chemical compounds that they consume and excrete(Germerodt et al. 2016; Hibbing et al. 2010). Does accounting for metabolism and diffusion suffice to predict the variation in colony growth? Genome-scale metabolic models and flux balance analysis can quantitatively predict the metabolites that microbes consume and excrete, and therefore can predict the ecological interactions that emerge from intracellular mechanisms (Orth et al. 2010; Mahadevan et al. 2002; Harcombe et al. 2014). Further, diffusion of biomass and nutrients can be incorporated to predict system dynamics in structured environments (Harcombe et al. 2014). We therefore can test whether colony variation is purely a function of metabolism and diffusion by comparing computational predictions against experimental observations. If factors such as toxicity, signals or stochastic differences in lag time drive colony variation then the model, which does not take these effects into account, will do a poor job. Determining the extent to which metabolic mechanisms drive spatial effects will be critical for predicting growth in complex natural settings.

Here we investigated how location influences interactions in arguably the simplest scenario – monocultures grown on homogeneous surfaces. We plated monocultures of either *Escherichia coli* or *Salmonella enterica* on various media and used high-resolution scanners to investigate

the size of colonies and the associated variance within each plate. We then used simulations and geometric descriptions of varying complexity to determine how much of the colony variation could be explained by metabolic mechanisms, what aspect of location best explained variation in growth, and how variation was influenced by changes in either nutrient uptake or diffusion. Finally, we investigated one case in which variation differed from expectation and suggest that this deviation was caused by byproduct toxicity. Our work provides a quantitative framework for understanding and predicting the effect of location on colony growth which is independent of both microscopic parameters and knowledge of the positions of the non-nearest neighbors.

Methods

Strains and media

We used cells of either *Salmonella enterica* subsp. *Typhimurium* LT2 or *Escherichia coli* K12-MG1655 as our model species. In the genome-scale metabolic modeling, these strains were represented by the iRR_1083 model (Raghunathan et al. 2009) and the ijo_1366 model (Orth et al. 2011), respectively. The Petri dish experiments either used LB media (10g/L tryptone, 10g/L NaCl, 5g/L yeast extract) or a modified Hypho minimal media (7.26mM K_2HPO_4, 0.88 mM NaH_2PO_4, 3.78 mM $[NH_4]_2SO_4$, 0.41 mM $MgSO_4$, 1 ml of a metal mix (Delaney et al. 2013)), with either glucose (8.34 mM), citrate (5.10 mM), lactose (4.17 mM), or acetate (12.5 mM) as the limiting resource. All Petri dishes had 1% agar. Dishes were left open under UV for 30 minutes.

For Petri dish experiments, cells from a 1-day old colony were used. After spreading cells onto a Petri dish, a thin piece of black plastic was placed within the upper lid of the dish to improve contrast and

reduce reflections from the Petri dish lid. Petri dishes were then placed onto a Canon Perfection V600 scanner agar side down and a 600dpi image was scanned every 20 minutes for almost 150 hours. Each treatment (a unique combination of a species and a media type) was repeated 4-8 times.

Image Analysis

Tracking of colony areas over time was performed in three main steps using custom software in Matlab (Supplementary material). First, the initial colony locations were detected. Then, the final colony areas were measured and merged colonies were separated (Fig. 1A). Finally, using the outlines of the final colony areas, the area of each colony was tracked through time. We measured the growth rate of colonies on Petri dishes via the diameter of a hypothetical circular colony with same area(Wimpenny 1979). The growth rate was calculated by regressing diameter over time for the first four hours (12 frames) once growth was detected.

Computational Modeling

All simulations were run in COMETS, a platform developed to do spatially-explicit dynamic flux-balance analysis simulations with an arbitrary number of species (Harcombe et al. 2014). Simulations were carried out using the University of Minnesota Supercomputing Institute's Mesabi cluster. COMETS uses dynamic flux balance analysis to predict bacterial growth over time by maximizing the amount of biomass which can be produced by a species' metabolic model given the resources in the local environment (Mahadevan et al. 2002). Michaelis-Menten kinetics constrain resource uptake, with the maximum set by v_{max} and the concentration at which uptake is at half-maximum set by k_m. In addition, we ran simplified reaction-diffusion simulations in COMETS by using a metabolic model with a single carbon uptake reaction, paired with a reaction that converted all intracellular carbon directly to biomass. In this simplified case uptake kinetics exactly match growth kinetics.

157

158 COMETS simulates growth in spatially-explicit environments by solving dynamic flux balance analyses in
159 discrete "boxes" within a lattice at each time step, and then allowing diffusion of the resources and
160 biomass among boxes between time steps. Each box can contain different amounts of biomass or
161 resources, which determine the outcome of the dynamic flux balance analysis. Biomass and resources
162 each diffuse to neighboring boxes with specific diffusion coefficients. The time-step and box sizes we
163 used were small enough to not cause a change in results if we reduced these sizes further.

164

165 The starting conditions, and length of time the simulations ran, depended on the question of interest.
166 For the simulations in figures 3 and 4 the "world" was a 5 cm x 5 cm square, into which 60 colonies were
167 seeded at random locations, with initial biomasses of 1e-10 grams. Resources were distributed
168 uniformly at a concentration of 1e-6 mmol per box for the limiting resource, and at essentially infinite
169 abundance for non-limiting resources. These simulations were run until resources were fully consumed.
170 The genome-scale metabolic model simulations, Fig. 2, were conducted in circular environments that
171 were 90 mm in diameter to mimic the experimental conditions. Biomass was seeded at the same
172 location as observed in experiments, and the concentration of the limiting resource also matched the
173 laboratory conditions. Genome-scale simulations were run for equal lengths of time as the laboratory
174 experiments. Other simulation parameters are provided in Table 1.

175

176 *Statistics*

177 The Voronoi areas and other distance metrics (nearest neighbor, summed inverse distances, summed
178 squared inverse distance) were all calculated in R. To find the Voronoi areas of colonies, we used the
179 spatstat package in R and ran the dirichletArea function. After calculation of any distance metric,

colonies <5mm from a Petri dish edge were excluded, i.e., the colonies were not included in the analysis, but they did contribute to the distance metric for included colonies.

We used relative metrics to compare yields between treatments and between experiments and simulations. We compared variation in colony yield on different carbon sources by first calculating the coefficient of variation in colony area for each Petri dish, then used a single factor ANOVA to compare the coefficient of variation between experimental treatments. Similarly, to compare experiment to simulation the yields at the end of growth, in units of area for the experiments and grams for the simulations, were divided by the total yield in each Petri dish or simulation area to obtain dimensionless values that could be directly compared. The experimental relative yields were compared with the simulation predictions using mixed-effects linear regression, with the Petri dish as a random factor and the treatment as a fixed factor.

To compare the strength of spatial competition among groups (media type, resource quality), we did an ANOVA followed by Tukey's Honest Significant Difference multiple comparisons test. The level of replication was the Petri dish. We conducted a t-test to test whether adding acetate to *S. enterica* Petri dishes with glucose altered the strength of spatial competition.

Results

The amount of variation in size between colonies on a surface depends on the resources and species identity

We tested whether species and resource identity influenced the variance in colony size within

monoculture plates. Approximately 60 cells of either *S. enterica* or *E. coli* were grown on 1% agar Petri dishes with different carbon sources, with 4-8 dishes per treatment. Colony areas were measured using flatbed scanners and custom software (Fig. 1A, see methods for more detail). Within every plate/replicate and treatment we found a range of colony sizes, as seen in the example density plots of the final colony areas in Fig. 1B, suggesting location was important for size variation. Because the *average* colony size differed substantially across treatments (see, for example, Fig. 1B), we used the coefficient of variation of final colony area (standard deviation over mean) within a plate to compare variation in colony size between treatments. Differences in media and species caused large differences in the coefficient of variation across treatment (ANOVA, $F(7,32) = 18.9$, $p = 1.07e\text{-}9$, Fig. 1C), suggesting that spatial effects were highly context dependent.

The effects of resource and species identity on the variance in colony size can be predicted with models that pair metabolism and diffusion.

We tested whether the observed variations in colony size could be predicted from the interplay of intracellular metabolic mechanisms, diffusion, and colony location, by running simulations that combine genome-scale metabolic modeling with diffusion calculations. Our computational platform, COMETS, uses dynamic flux-balance analysis to predict the growth and metabolic activity of bacteria by identifying the metabolic strategy that maximizes biomass production at each time step (Mahadevan et al. 2002; Harcombe et al. 2014). Biomass and metabolites diffuse to simulate growing colonies and the resource gradients that arise as a result of

226 microbial metabolism. Note that this does not mean that colonies spread by diffusion alone
227 from the center of the colony. Rather, the combined action of diffusion and growth leads to
228 biomass spread (Murray 2002).
229
230 Simulations were initiated with resources and colony locations that matched each experimental
231 plate (Fig. 2A). We plotted the relative yields (yield of a colony / total yield on a Petri dish) for
232 simulations against those for experiments (Fig. 2B). We used relative yields because the
233 measurements of interest were the relative differences between colonies on a plate, which can
234 be compared with relative numbers even if the specific yield measurement (area vs biomass)
235 differs. The relative colony sizes in simulations were well correlated with the relative colony
236 sizes in experiments, although the predictive ability of the simulations depended on the
237 treatment (mixed-effects linear regression with subsequent F tests, main effect of simulated
238 yields: $F(1,1479) = 2027$, $p < 2.2e\text{-}16$, main effect of treatment: $F(5,24) = 11$, $p = 1.3e\text{-}5$,
239 interaction: $F(5,1470) = 85$, $p < 2.2e\text{-}16$). Deviations from simulated predictions had a slope < 1,
240 meaning there was more variability in colony size in simulations than in experiments, which
241 occurred and was most pronounced when the carbon resource was a sugar (i.e. glucose or
242 lactose). Below we further explore the deviations caused by growth on sugars.
243
244 *Relative colony size is driven by the location of adjacent competitors*
245
246 To more extensively investigate how location determines colony size we simplified our model
247 to allow faster simulation and abstract species/environment-specific intracellular metabolism.

We replaced the genome-scale metabolic model with a set of differential equations, which describe a reaction-diffusion system in which bacteria grow under Monod kinetics: The growth rate f(B,R) depends on biomass concentration B and resource concentration R. Bacteria and resource spread via diffusion, with the diffusion coefficient for the bacteria D_B being much smaller than that for the resource, D_R (equations 1):

$$\frac{\partial B}{\partial t} = D_B \nabla^2 B + f(B,R) \quad (1a)$$

$$\frac{\partial R}{\partial t} = D_R \nabla^2 R - f(B,R) \quad (1b)$$

$$f(B,R) = B\frac{v_{max} R}{k_m + R} \quad (1c)$$

The first term in each of the differential equations describes diffusion (∇^2 is the two-dimensional Laplacian operator.), the second term (the "reaction" term) describes conversion of the resource into biomass which occurs with the same efficiency independent of the growth rate. The maximum growth rate, v_{max}, is approached as the resource concentration R increases, with half-maximum growth rate attained when the resource concentration is equal to the saturation constant k_m.

With this model, we sought a distance-based metric that could predict colony size independently of intracellular details, focusing on metrics that had previous use in the forestry or microbiology literature(Tome & Burkhart 1989; Guillier et al. 2006; Lloyd & Allen 2015). We first simulated conditions that caused strong spatial effects (large variance in colony size), which used a high growth rate (v_{max} = 1). We tested whether colony size could be best predicted by the distance to the nearest neighbor (Fig. 3A), the sum of the inverse distances to all neighbors (Fig. 3B), the log of the sum of the squared inverse distances (Fig. 3C), or a colony's Voronoi area, which is the area on the Petri dish which is closer to the focal colony than to any other colony (Fig. 3D)(Okabe et al. 2000). While all metrics were somewhat predictive of colony size, the Voronoi areas had almost perfect prediction.

To further test whether Voronoi neighbors are the primary competitors, we ran "dropout" simulations, in which we repeatedly simulated the same environment (i.e. founding cell locations) but removed a different seed of a colony from each simulation. We then determined the impact that each removal had on focal colony sizes, to test the effect of removing a Voronoi neighbor vs. a non-Voronoi neighbor. Removing Voronoi neighbor colonies had much larger effects than removing non-Voronoi neighbors, Fig. 3F (t.test, p = 5.6e-7). Taken together, this means that colonies that determined territory boundaries (the Voronoi neighbors) played the most important role in causing spatial effects.

Finally, we tested the relative predictive ability of Voronoi areas as spatial effects decreased. We repeated the metric comparison at increasing resource diffusion coefficients D_R, spanning

a range that at the low end is similar to the diffusion coefficient of a large protein such as bovine serum albumin in 1% agar (~1E-7 cm^2 / s), passing the typical diffusion coefficient for sugars (~5E-6 cm^2 / s), and reaching past the diffusion coefficient of sodium choride (~1.5E-5 cm^2 / s) (Schantz & Lauffer 1962). Even as the resource diffusion coefficient increased, causing competition to become more global (described below), the Voronoi areas were still the best predictors of yields (Supp. Fig 1). Therefore, we concluded that the territory closest to a colony, obtained using a Voronoi diagram and determined by the competitors which are in adjacent Voronoi areas, is generally the best predictor for how competition for diffusing resources affects colony size.

The influence of Voronoi neighbors is determined by the competing effects of resource uptake and diffusion

Our results above show that Voronoi area is the best metric for capturing the effect of location on colony size, so we next used this metric to investigate how diffusion and resource usage parameters influence the strength of spatial effects. To analyze the impact of diffusion and uptake we focused on the slope of the line that is generated when plotting $\frac{yield_i}{\sum yield}$ against $\frac{Voronoiarea_i}{totalarea}$, for individual colonies. If each colony has exclusive access to the resources in its territory, the plot should generate a line with a slope of 1. A smaller slope represents increased movement of resources between Voronoi areas. For example, if a plot of $\frac{yield_i}{\sum yield}$ over $\frac{Voronoiarea_i}{totalarea}$ yields a line with a slope of 0.5, a two-fold increase in a colony's Voronoi area only

allows that colony to consume one-fold more resources (since all resources all turned into biomass, independent of rate). In a situation where the slope equals 0, the yield of colonies is largely the same and independent of Voronoi areas (Fig. 4A). Intuitively, a decrease in the slope should occur as competition becomes more global. These interpretations are consistent with the observation that a decrease in the slope, which we deemed the "relative effect of Voronoi area", goes along with a decrease in the yield coefficient of variation and the R^2 of the plot (Fig. 4B) when varying any parameter (v_{max},k_m, R, D_B, or D_R). The correlation between these metrics indicates that parameters that reduce the slope also reduce the amount of variation in colony size and the predictive ability of Voronoi areas.

We next tested what parameters in the model altered the relative effect of Voronoi area. Increasing the rate at which colonies consume nutrients increased the relative effect of Voronoi area. The effects of changing the upper limit on uptake rate (Vmax), the saturation constant (km), or the initial resource concentration (R) all collapsed into a single effect, the maximum uptake rate, by calculating the Monod maximum uptake using Vmax * R / (km + R) (Figure 4C). Increasing the maximum uptake rate caused a fast increase in the relative effect of Voronoi areas until saturating.

We next investigated the influence of biomass and resource diffusion. Increasing the biomass diffusion coefficient (D_B) increased the relative effect of Voronoi area (Fig. 4D). We hypothesize this effect was due to a concomitant increase in the rate at which colonies took up resources that occurred because colonies spread more quickly and were able to reach high

334 resource concentration zones faster. In otherwise identical simulations, faster biomass diffusion
335 did increase the speed at which resources were consumed (Supp. Fig 2).
336
337 In contrast to the effect of resource uptake and biomass diffusion, increasing resource diffusion
338 (D_R) *reduced* the relative effect of Voronoi areas. As the resource diffusion coefficient
339 increases, the relative impact of Voronoi neighbors decays (Fig. 4E) likely because diffusion
340 outpaces resource uptake. As a result the impact of Voronoi neighbors is determined by the
341 interplay of nutrient uptake and diffusion (Fig 4 F).
342
343 *In laboratory experiments, growth rate predicts the relative effect of Voronoi area*
344
345 We tested the predicted explanatory power of growth parameters on our laboratory data from
346 Fig. 1. In every treatment, the colony sizes scaled with the colonies' Voronoi area, as seen in the
347 scatterplots with data from four Petri dishes per treatment shown in Fig. 5A. The relative effect
348 of Voronoi area depended on the species and the environment, Fig. 5B (two-way ANOVA, effect
349 of media: $F(4,36) = 40.6$, $p < 1e\text{-}10$), no main effect of species, interaction between
350 media:species: $F(2,36) = 5.88$, $p = 0.0062$).
351
352 In simulations, the maximum growth rate and resource uptake rate were directly proportional,
353 and we showed than increasing the maximum uptake rate increased the relative effect of
354 Voronoi area. In the laboratory data, we measured the maximum growth rate as the increase in
355 diameter over the first three hours after colonies were identified(Palumbo et al. 1971). Media

and species each caused significant differences in the maximum growth rate, Fig. 5C (ANOVA, effect of media: $F(4,38) = 260$, $p < 2e\text{-}16$, effect of species: $F(1,38) = 28.2$, $p = 5.1e\text{-}6$). Furthermore, in agreement with simulations, the relative effect of Voronoi area in laboratory experiments increased as maximum growth rate increased following a saturating function (Fig. 5C). However, there was the appearance of an outlier: *S. enterica* grown on glucose.

S. enterica grown on glucose appeared not to follow the growth rate—Voronoi effect trend (Fig. 5C), and also was the treatment most poorly predicted by the genome-scale metabolic modeling (Fig. 2B). This led us to hypothesize that another biological phenomenon besides competition for diffusing resources was occurring in this treatment. Interestingly, Voronoi areas and metabolic models did a good job of predicting the size of small colonies however, large colonies were routinely smaller than predicted (Fig. 2B). This suggests that large colonies stopped growing before they ran out of resources. *S. enterica* can generate potentially-toxic acetate during growth on glucose, so we hypothesized that acetate accumulation arrested growth of large colonies (Cappuyns et al. 2009; Wolfe 2005; Rhee et al. 2003). To test this hypothesis we grew *S. enterica* on Petri dishes with glucose medium with or without supplemented acetate (each at the same concentration as used in single carbon cultures), reasoning that if acetate was accumulating and causing toxicity, thereby reducing the spatial effects, supplementing acetate would further reduce the spatial effect. Consistent with our hypothesis supplemental acetate (but not growth on acetate alone) reduced the growth of the colonies (Fig. 6A) and the relative effect of Voronoi area (Fig. 6B). Furthermore, genome-scale metabolic modeling (which does not model toxicity) better recapitulated the laboratory data at

an earlier time point, when less acetate would have accumulated. This was true for *S. enterica* on glucose, as well as for *E. coli* on glucose or lactose, each of which can cause acetate accumulation (Fig. 6C) (Wolfe 2005).

Discussion

Understanding the quantitative way that spatial proximity affects interactions between bacterial colonies will allow us to better understand and manage microbial ecosystems. We showed that while species identity and the resources present caused variations in the effect of colony proximity, we could nevertheless predict much of this variance using models accounting for metabolism and diffusion. Spatially-dependent variation in colony size was largest on media which promoted a fast growth rate. Specific colony sizes were best predicted using Voronoi diagrams, which means that the differential colony growth was primarily caused by adjacent competitors (the "Voronoi neighbors") (Okabe et al. 2000). The specific influence of these Voronoi neighbors was determined by a balance between the rate at which colonies took up resources, and resource diffusion. High uptake rates increased the importance of Voronoi neighbors and caused greater spatially-dependent variance in colony size. This general ecological relationship held across species and environments and therefore serves as a useful null model from which to predict spatial effects caused by resource competition. We demonstrated the utility of this null model: experiments in which Voronoi neighbors had less influence than would be predicted from growth rate led us to suggest that the toxicity of organic acid byproducts plays an important role in limiting colony size when bacteria are growing on sugars. In summary, we provide an experimentally and theoretically grounded

400 understanding of how location interacts with metabolism and diffusion to influence microbial
401 interactions.
402
403 We found that the impact of location on microbial growth was strongly influenced by both
404 species and resource identity. This finding highlights the fact that the impact of spatial structure
405 is context-dependent. While a dichotomy between structured and unstructured environments
406 has value (Kim et al. 2008; Kerr et al. 2002; Chao & Levin 1981), it is important to realize that
407 the effect of structure can change dramatically in different environments (Allen et al. 2013). As
408 we strive to understand interaction strengths in natural microbial communities and design
409 spatially-structured ecosystems for technological applications, it will be vital to incorporate
410 context-dependent effects of location.
411
412 Encouragingly, spatially-explicit, genome-scale metabolic models were able to predict much of
413 the variation in colony size by modeling the interaction between diffusion and intracellular
414 metabolism. This suggests that with models created from sequence data we will be able to
415 quantitatively predict metabolic microbial interactions in complex, spatially structured
416 environments. High-throughput methods to generate models from sequence data are
417 improving(Feist et al. 2009), and therefore spatially explicit tools such as COMETS will be
418 increasingly useful to generate quantitative predictions of the effect of location on growth and
419 microbial interactions. As we discuss below, the accuracy of the predictions will be strongly
420 influenced by realized uptake rates. The upper-limit of uptake (Vmax) must be defined in the
421 model but will often be difficult to infer from sequence data. However, in our simulations we

left the upper-limit for all metabolites set at a canonical value of 10 mmol / gram dry weight / hr (Harcombe et al. 2014) and still achieved a good match between simulation and experiment. This suggests that colony-level uptake rates depended more on the stoichiometry of biomass production on each carbon source than on Vmax. Therefore, accurate predictions of stoichiometry, obtainable from sequence data, may lead to good approximations of the rate at which growing colonies consume resources even with inexact limits on uptake rates.

Voronoi diagrams did substantially better at explaining colony variance than did any of the other metrics that we tried. Dropout simulations show that colonies outside the Voronoi neighbors have very little influence on variation in colony size. Interestingly, this suggests that for competition the arrangement of nearby colonies matters more than the specific proximity of those colonies. One caveat of our findings is that all of our colonies started to grow at roughly the same time. Had bacteria colonized the plate at different time points, or varied dramatically in lag time, Voronoi diagrams would likely explain less of the variance. Indeed differences in lag time have been shown to influence competition for physical space (Lloyd & Allen 2015), however, lag time had exceedingly little impact on colony variance in our experiments (data not shown). Additionally, we only looked at interactions with conspecific colonies. We expect that predicting interactions between species with different resource uptake rates will require weighted Voronoi diagrams. Finally, in future work it will also be interesting to investigate how Voronoi diagrams fair in three-dimensional ecosystems, such as lung infection models (Connell et al. 2014).

444 A balance of resource uptake and diffusion determined the extent to which competitive
445 interactions between bacterial colonies were localized. Any parameter that increased uptake
446 increased the influence of Voronoi neighbors (up to a limit), but increasing resource diffusion
447 mitigated this effect. This means that both uptake and diffusion must be considered to
448 determine the extent to which interactions are local. One might expect non-localized
449 interactions in aquatic environments due to the low viscosity of the media, but if liquid is static,
450 and resource-rich, the bacteria nevertheless may interact primarily with Voronoi neighbors.
451 Conversely, in structured environments where one might expect highly localized interactions, if
452 nutrient uptake is slow enough, resource diffusion may overpower resource uptake and
453 globalize the interactions. It is important to note that decreasing the extent to which
454 competition is local is not equivalent to decreasing competition. The average colony size and
455 total biomass on a plate are equivalent whether competition is local or global (assuming all
456 resources are consumed). However, if the balance of uptake and diffusion cause interactions to
457 be local, spatial location matters, and some colonies will grow much larger than others.
458
459 The balance between resource uptake and diffusion provides a null model for colony variance
460 given resource competition in a spatial environment. If colony growth is mediated by
461 competition for relatively slowly diffusing resources, then colony size should correlate with
462 Voronoi area. Departures from this null expectation can help identify circumstances in which
463 other biological interactions are occurring. In our experiments, colony size of *S. enterica*
464 correlated poorly with Voronoi area when glucose was the carbon source, despite a fast rate of
465 growth. Here, waste accumulation appears to have stunted the growth of large colonies. Both

E. coli and *S. enterica* produce organic acids as a byproduct of growth on sugars, and acetate toxicity can hinder growth(Wolfe 2005; Vandenbergh 1993). This toxicity reduced the relative importance of location. As production of toxic byproducts is common in the microbial world, it will be interesting to further investigate how toxicity influences spatial patterns. More broadly, the detection of toxicity in our system serves as an example of how quantitative analysis can aid in the identification of species interactions. Different biological phenomena likely cause specific departures from the null expectations. For instance, we hypothesize that mutualistic interactions between colonies will cause spatial effects, but of opposite direction to competition, in which colonies in smaller Voronoi areas have better success. Further research will be aimed at finding signatures of these and other biological phenomena.

A quantitative understanding of how location mediates microbial interactions has important consequences for understanding and harnessing microbial evolutionary ecology. It is well established that spatial structure matters, can alter the interactions between microbes(Nadell et al. 2016) and plays a critical role in determining health outcomes(Stacy et al. 2016). Quantifying how space mediates interactions will allow for more rigorous understanding of community composition, and improve prediction of dynamics such as competitive exclusion. Further, understanding organisms' interaction strengths is critical for understanding the evolution of microbial traits. For example, it was recently demonstrated that the level of antibiotic secretion can be explained by the relative strength of interaction with sensitive and resistant competitors (Gerardin et al., 2016). As technology which allows for fine-scale placement of cells matures (Xu et al. 2004; Ferris et al. 2013; Connell et al. 2013), we can create

488 spatial arrangements that maximize selection of competitive phenotypes of interest. As we
489 strive to move beyond descriptions of microbial diversity to explanations and management of
490 diversity it will be critical to develop quantitative understanding of microbial interactions.
491

Acknowledgements The authors thank S. Zhuang for advice on the scanning technique and the UMN theory group for useful discussions. J. Chacón was funded by the Biocatalysis Initiaitive through UMN.

References

Allen, B., Gore, J. & Nowak, M.A., 2013. Spatial dilemmas of diffusible public goods. *eLife*, 2013(2), pp.1–11.

Allison, S.D., 2005. Cheaters, diffusion and nutrients constrain decomposition by microbial enzymes in spatially structured environments. *Ecology Letters*, 8(6), pp.626–635.

Arrigo, K.R., 2005. Marine microorganisms and global nutrient cycles. *Nature*, 437(7057), pp.343–348.

Cappuyns, A.M. et al., 2009. A dynamic model for diauxic growth, overflow metabolism, and AI-2-mediated cell-cell communication of Salmonella Typhimurium based on systems biology concepts. *Biotechnology and Bioengineering*, 102(1), pp.280–293.

Chao, L. & Levin, B.R., 1981. Structured habitats and the evolution of anticompetitor toxins in bacteria. *Proceedings of the National Academy of Sciences of the United States of America*, 78(10), pp.6324–6328.

Cho, I. & Blaser, M.J., 2012. The human microbiome: at the interface of health and disease. *Nature Reviews Genetics*, 13(4), pp.260–270. Available at: http://dx.doi.org/10.1038/nrg3182.

Connell, J.L. et al., 2013. 3D printing of microscopic bacterial communities. *Proceedings of the National Academy of Sciences of the United States of America*, 110(46), pp.18380–18385. Available at: http://www.pnas.org/content/110/46/18380.full%5Cnpapers3://publication/doi/10.1073/pnas.1309729110.

Connell, J.L. et al., 2014. Real-time monitoring of quorum sensing in 3D-printed bacterial aggregates using scanning electrochemical microscopy. *Proceedings of the National Academy of Sciences of the United States of America*, 111(51), pp.18255–60. Available at: http://www.pnas.org/lookup/doi/10.1073/pnas.1421211111%5Cnhttp://www.ncbi.nlm.nih.gov/pubmed/25489085.

David, L.A. et al., 2015. Gut Microbial Succession Follows Acute Secretory Diarrhea in Humans. *mBio*, 6(3), pp.1–14.

Dechesne, A., Or, D. & Smets, B.F., 2008. Limited diffusive fluxes of substrate facilitate coexistence of two competing bacterial strains. *FEMS Microbiology Ecology*, 64(1), pp.1–8.

Delaney, N.F. et al., 2013. Development of an Optimized Medium, Strain and High-Throughput Culturing Methods for Methylobacterium extorquens. *PLoS ONE*, 8(4).

Feist, A.M. et al., 2009. Reconstruction of Biochemical Networks in Microbial Organisms. *Nature Reviews Microbiology*, 7(2), pp.129–143.

Ferris, C.J. et al., 2013. Biofabrication: An overview of the approaches used for printing of living cells. *Applied Microbiology and Biotechnology*, 97(10), pp.4243–4258.

Foster, K.R. & Bell, T., 2012. Competition, not cooperation, dominates interactions among culturable microbial species. *Current Biology*, 22(19), pp.1845–1850. Available at: http://dx.doi.org/10.1016/j.cub.2012.08.005.

Gandhi, S.R. et al., 2016. Range expansions transition from pulled to pushed waves as growth becomes more cooperative in an experimental microbial population. *Proceedings of the National Academy of Sciences*, 113(25), pp.6922–6927. Available at: http://www.pnas.org/lookup/doi/10.1073/pnas.1521056113.

Gerardin, Y., Springer, M. & Kishony, R., 2016. A competitive trade-off limits the selective advantage of increased antibiotic production. *Nature Microbiology*, 1(September), p.16175. Available at:

http://www.nature.com/articles/nmicrobiol2016175.

Germerodt, S. et al., 2016. Pervasive Selection for Cooperative Cross-Feeding in Bacterial Communities. *PLoS Computational Biology*, 12(6), pp.1–21.

Gralka, M. et al., 2016. Allele surfing promotes microbial adaptation from standing variation. *Ecology Letters*, 19(8), pp.889–898.

Greig, D. & Travisano, M., 2008. Density-dependent effects on allelopathic interactions in yeast. *Evolution*, 62(3), pp.521–527.

Guillier, L., Pardon, P. & Augustin, J.C., 2006. Automated image analysis of bacterial colony growth as a tool to study individual lag time distributions of immobilized cells. *Journal of Microbiological Methods*, 65(2), pp.324–334.

Hallatschek, O. et al., 2007. Genetic drift at expanding frontiers promotes gene segregation. *Proceedings of the National Academy of Sciences of the United States of America*, 104(50), pp.19926–30. Available at: http://www.pnas.org/content/104/50/19926.long.

Hallatschek, O. & Nelson, D.R., 2010. Life at the front of an expanding population. *Evolution*, 64(1), pp.193–206.

Hansen, S.K. et al., 2007. Evolution of species interactions in a biofilm community. *Nature*, 445(7127), pp.533–536.

Harcombe, W.R. et al., 2014. Metabolic resource allocation in individual microbes determines ecosystem interactions and spatial dynamics. *Cell Reports*, 7(4), pp.1104–1115.

Hibbing, M.E. et al., 2010. Bacterial competition: surviving and thriving in the microbial jungle. *Nature reviews: Microbiology*, 8(JaNuary), pp.15–25.

Kerr, B. et al., 2002. Local dispersal promotes biodiversity in a real-life game of rock-paper-scissors. *Nature*, 418(6894), pp.171–174.

Kim, H.J. et al., 2008. Defined spatial structure stabilizes a synthetic multispecies bacterial community. *Proceedings of the National Academy of Sciences of the United States of America*, 105(47), pp.18188–18193.

Korolev, K.S. et al., 2012. Selective sweeps in growing microbial colonies. *Physical Biology*, 9(2).

Lloyd, D.P. & Allen, R.J., 2015. Competition for space during bacterial colonization of a surface. *Journal of The Royal Society Interface*, 12(110), p.20150608. Available at: http://rsif.royalsocietypublishing.org/lookup/doi/10.1098/rsif.2015.0608.

Mahadevan, R., Edwards, J.S. & Doyle 3rd, F.J., 2002. Dynamic flux balance analysis of diauxic growth in Escherichia coli. *Biophys J*, 83(3), pp.1331–1340. Available at: http://dx.doi.org/10.1016/S0006-3495(02)73903-9.

Mitri, S., Clarke, E. & Foster, K.R., 2015. Resource limitation drives spatial organization in microbial groups. *The ISME Journal*, 10(6), pp.1–12. Available at: http://dx.doi.org/10.1038/ismej.2015.208.

Mitri, S. & Foster, K.R., 2013. The genotypic view of social interactions in microbial communities. *Annu Rev Genet*, 47, pp.247–273. Available at: http://www.ncbi.nlm.nih.gov/pubmed/24016192.

Momeni, B. et al., 2014. Strong inter-population cooperation leads to partner intermixing in microbial communities. *eLife*, 3, p.e02945.

Murray, J.D. (James D., 2002. *Mathematical biology 1, An introduction*, Springer.

Nadell, C.D., Drescher, K. & Foster, K.R., 2016. Spatial structure, cooperation, and competition in biofilms. *Nature Reviews Microbiology*, accepted. Available at: http://dx.doi.org/10.1038/nrmicro.2016.84.

Okabe, A. et al., 2000. *Spatial tesselations: concepts and applications of Voronoi diagrams* 2nd ed., New York, NY: John Wiley & Sons.

Orth, J.D. et al., 2011. A comprehensive genome-scale reconstruction of Escherichia coli metabolism--2011. *Molecular systems biology*, 7(535), p.535. Available at: http://www.pubmedcentral.nih.gov/articlerender.fcgi?artid=3261703&tool=pmcentrez&rendertyp

588 e=abstract.
589 Orth, J.D., Thiele, I. & Palsson, B.Ø., 2010. What is flux balance analysis? *Nature biotechnology*, 28(3),
590 pp.245–248. Available at: http://dx.doi.org/10.1038/nbt.1614.
591 Palumbo, S. a et al., 1971. Growth measurements on surface colonies of bacteria. *Journal of general*
592 *microbiology*, 66(2), pp.137–143.
593 Penn, A.S. et al., 2012. Can Simpson's paradox explain co-operation in Pseudomonas aeruginosa
594 biofilms? *FEMS Immunology and Medical Microbiology*, 65(2), pp.226–235.
595 Persat, A. et al., 2015. The mechanical world of bacteria. *Cell*, 161(5), pp.988–997. Available at:
596 http://dx.doi.org/10.1016/j.cell.2015.05.005.
597 Pirt, S.J., 1967. A Kinetic Study of the Mode of Growth of Surface Colonies of Bacteria and Fungi. *Journal*
598 *of general Microbiology*, 47, pp.181–197.
599 Raghunathan, A. et al., 2009. Constraint-based analysis of metabolic capacity of Salmonella typhimurium
600 during host-pathogen interaction. *BMC Systems Biology*, 3, p.38. Available at:
601 papers3://publication/doi/10.1186/1752-0509-3-38.
602 Rhee, M. et al., 2003. Antimicrobial Effects of Mustard Flour and Acetic Acid against Escherichia coli
603 Salmonella enterica Serovar Typhimurium Antimicrobial Effects of Mustard Flour and Acetic Acid
604 against Escherichia coli O157 : H7 , Listeria monocytogenes , and Salmonella ent. *Appl. Environm.*
605 *Microbiol.*, 69(5), pp.2959–2963.
606 Schantz, E.J. & Lauffer, M.A., 1962. Diffusion Measurements in Agar Gel. *Biochemistry*, 1(4), pp.658–663.
607 Available at: http://dx.doi.org/10.1021/bi00910a019.
608 Shade, A. et al., 2012. Fundamentals of microbial community resistance and resilience. *Frontiers in*
609 *Microbiology*, 3(DEC), pp.1–19.
610 Stacy, A. et al., 2014. Bacterial fight-and-flight responses enhance virulence in a polymicrobial infection.
611 *Proceedings of the National Academy of Sciences of the United States of America*, 111(21),
612 pp.7819–24. Available at:
613 http://www.pubmedcentral.nih.gov/articlerender.fcgi?artid=4040543&tool=pmcentrez&rendertyp
614 e=abstract.
615 Stacy, A. et al., 2016. The biogeography of polymicrobial infection. *Nature Reviews Microbiology*, 14(2),
616 pp.93–105. Available at:
617 http://www.nature.com/nrmicro/journal/v14/n2/full/nrmicro.2015.8.html%5Cnhttp://www.natur
618 e.com/nrmicro/journal/v14/n2/pdf/nrmicro.2015.8.pdf.
619 Tome, M. & Burkhart, H.E., 1989. Distance-dependent competition measures for predicting growth of
620 individual trees. *Forest Science*, 35(3), pp.816–831.
621 Vandenbergh, P., 1993. Lactic acid bacteria, their metabolic products and interference with microbial
622 growth. *FEMS Microbiology Reviews*, 12(1–3), pp.221–237. Available at:
623 http://www.sciencedirect.com/science/article/pii/016864459390065H.
624 Wimpenny, J.W.T., 1979. The growth and form of bacterial colonies. *J Gen Microbiol*, 114(2), pp.483–
625 486. Available at: http://www.ncbi.nlm.nih.gov/pubmed/120410.
626 Wolfe, A.J., 2005. The Acetate Switch The Acetate Switch. *Microbiology and Molecular Biology Reviews*,
627 69(1), pp.12–50.
628 Xu, T. et al., 2004. Construction of High-Density Bacterial Colony Arrays and Patterns by the Ink-Jet
629 Method. *Biotechnology and Bioengineering*, 85(1), pp.29–33.
630

Figure Legends

Figure 1: The variance in colony yields depends on the species and environment

A) A snapshot of *S. enterica* colonies on LB media (left) and the yields (areas) of those colonies determined by automated image analysis (right). B) Density distributions of *S. enterica* colony yields grown on acetate or LB. C) The coefficient of variation of colony yields for each species on each carbon course. Error bars are standard error of mean.

Figure 2: Genome-scale metabolic modeling recapitulates the variance in colony yields

A) We used genome-scale metabolic modeling in the COMETS platform to test the mechanisms generating the observed variance in colony yields. The relevant genome-scale metabolic model was seeded into an environment at the sites from which colonies initiated in experiments. Dynamic flux-balance-analysis calculations and subsequent metabolite and biomass diffusion were carried out in discrete time steps for a duration mimicking the laboratory experiments. B) A comparison of the relative colony yields measured in experiments (y axis) to the relative colony yields predicted by the COMETS simulations (x axis) for the treatments accessible with COMETs (defined media, i.e. not LB). Each facet contains data from 4-8 Petri dish experiments / simulations. The black line has slope = 1 and intercept = 0, while the blue lines and surrounding grey are linear regression lines with standard error. A high R^2 suggests that the relative spatial effects are captured by the model, while a slope close to 1 suggests an accurate prediction of amount of variance in colony yield.

Figure 3: Voronoi diagrams capture the effect of location on yield better than other distance metrics

Four metrics were tested to determine which colonies interact to generate variation in colony size and to what extent. A-D show a cartoon of the measurement and the metric plotted against simulated colony yield (biomass). A) The distance to the closest colony, such that the yield of the focal colony (indicated by the arrow) would be predicted from the distance to colony 1, which is closest, but no other colony would be considered. B) The inverse linear distance to every colony, such that the yield of the focal colony would be predicted by the distance to every colony, with each colony's influence inversely proportional to its distance. C) Like B, but colonies become quadratically less important as distance increases. D) The territory closest to a colony, described by a Voronoi diagram. Here, the focal colony's Voronoi area is shown (solid line polygon). A Voronoi diagram divides a plane into areas around colony initiation sites such that all the space in a territory is closer to its enclosed colony than to any other colony, which is accomplished by drawing perpendicular lines half-way through lines connecting a focal colony to Voronoi neighbors. E) A Voronoi diagram drawn for all colony initiation sites on a Petri dish. For a focal colony (blue), its Voronoi neighbors are the green colonies. F) The percent increase in a focal colony's yield, after removal of a Voronoi or non-Voronoi neighbor. Error bars are standard error.

Figure 4: Colony resource uptake rate and resource diffusion determine the relative effect of Voronoi area

A) We quantified the relative effect of Voronoi area by measuring the slope of a line through the standardized colony biomass yields over the colonies' standardized Voronoi areas. A slope = 1 means that there are strong spatial effects and Voronoi neighbors exert total influence over a focal colony's

yield, whereas a slope = 0 means that all colonies exert similar effects regardless of spatial proximity and therefore competition is global. B) As relative effect of Voronoi area increases, so does the variance explained by the Voronoi areas (100 * R^2) and the coefficient of variation of colony yield when varying any model parameter. C) The relative effect of Voronoi area increases with the maximum potential per-mass uptake. Changes from the default (baseline) values (Table 1) in maximum growth rate, km, starting resource concentration, or any combination of these parameters (multiple) all have similar effects. D) The relative effect of Voronoi area increases as the biomass diffusion coefficient increases. E) The relative effect of Voronoi area decreases as resource diffusion increases. F) The relative effect of Voronoi area is determined by the balance between the maximum uptake rate of a colony (x axis) and the rate of resource diffusion (y axis).

Figure 5: The relative effect of Voronoi area changes between experimental treatments but generally scales with the maximum colony growth rate

A) Scatterplots of the yield of *S. enterica* colonies over their Voronoi areas when grown on citrate or LB media. B) The relative effect of Voronoi area varied from extremely low (*E. coli* on acetate) to high (either species on LB) in experiments. The gray dots are measurements from individual Petri dishes, and the black dots and bars are means and standard error of the means, respectively. C) The relative effect of Voronoi area plotted over the maximum growth rate. The black line is a fit to data, excluding data from *S. enterica* grown on glucose.

Figure 6: Acetate addition or accumulation reduces the relative effect of Voronoi area

A) *S. enterica* colonies grown on Petri dishes with glucose alone or with acetate added. The scalebar = 2.5mm. B) The relative effect of Voronoi area with only acetate, only glucose or a combination of the two. The gray dots are measurements from individual Petri dishes, and the black dots and bars are means and standard error of the means, respectively. C) The simulations from Fig. 2B, but with the simulated results taken from 40 hours into the simulation rather than at the end of the experiment (150 hrs). Acetate accumulation is not predicted to occur until 40 hours.

Supplementary Figure 1: Voronoi areas are the best predictors of yield even as the system becomes more global

The amount of yield variance explained by each metric as the resource diffusion rate is increased. The colony layout is the same as for the data in Fig. 3. Regardless of the diffusion rate, Voronoi areas are the superior metric.

Supplementary Figure 2: Total consumption of the ecosystem's resources occurs more quickly as the biomass diffusion coefficient increases

The time step at which 99.9% of the simulated ecosystems' resources were consumed, plotted over the biomass diffusion constant. All other parameters were held constant. The data is from the same simulations as shown in Fig. 4D.

721
722
723

Parameter	value	Unit, description
spaceWidth	0.05	Side length of a box, in cm
deathRate	0	Constant rate of biomass loss per hour
allowCellOverlap	True	Whether multiple colonies could share a box
minSpaceBiomass	1E-14	Minimum grams of biomass allowed in a box
maxSpaceBiomass	5E-3	Maximum grams of biomass allowed in a box
defaultVmax	1	mmol / gram / hour, max uptake rate or growth rate
defaultKm	0.005	mM, concentration of half-maximum uptake rate
exchangeStyle	Monod Style	Uptake is governed by monod kinetics
defaultDiffConst	5e-6	cm^2 / s, diffusion constant of resources / metabolites
flowDiffRate	3e-9	cm^2 / s, diffusion constant of bacterial biomass
numDiffPerStep	10	How many iterations to solve the diffusion equations per timestep
timeStep	0.1	Hours, amount of time per timestep
Resource concentration	1e-6	Mmols of resource initiated in a box

724 Table 1: Baseline COMETS parameters used for simulations

725

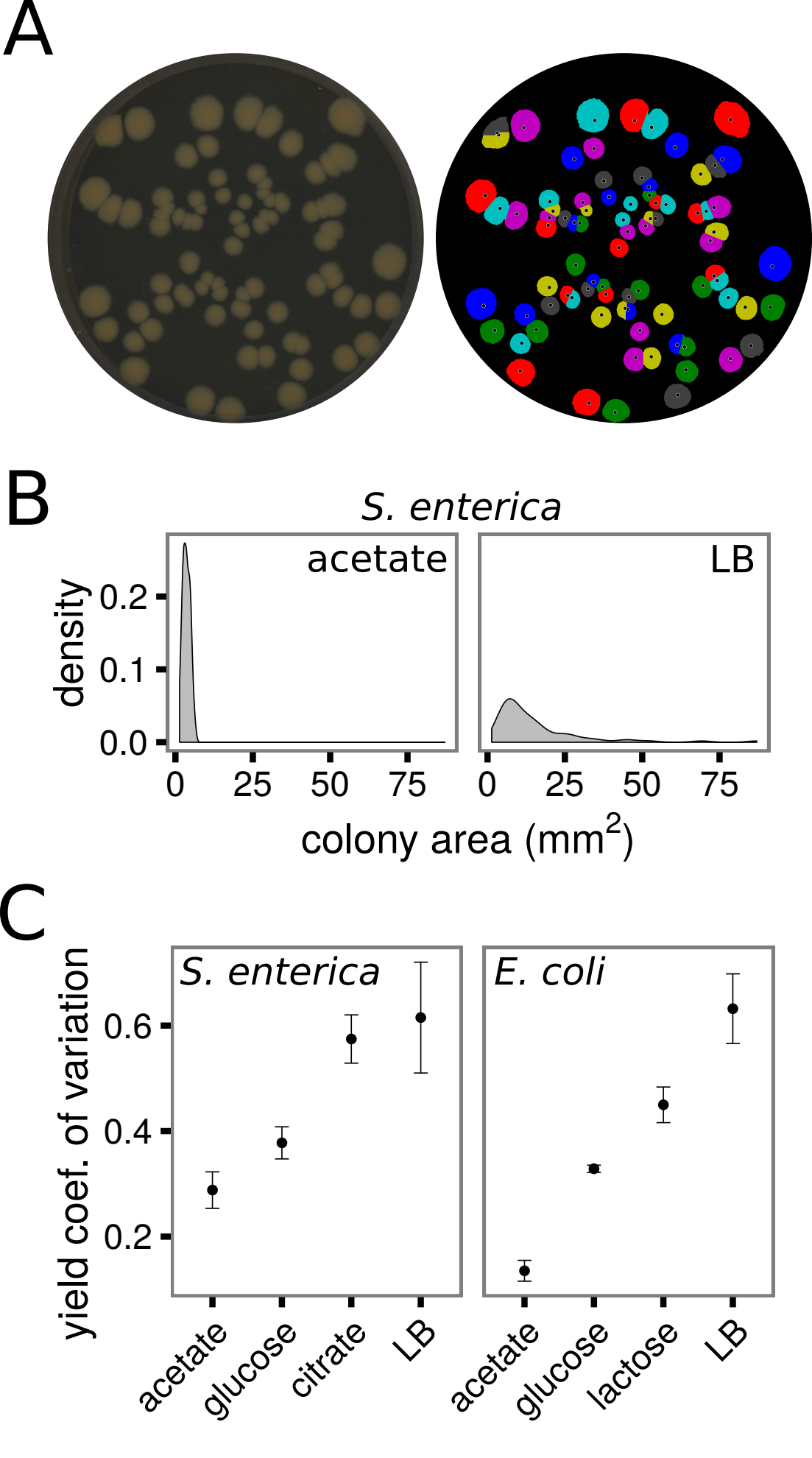
A
B
S. enterica
acetate
LB
density
0.2
0.1
0.0
0
25
50
75
colony area (mm2)
C
S. enterica
E. coli
yield coef. of variation
0.6
0.4
0.2
acetate
glucose
citrate
LB
acetate
glucose
lactose
LB

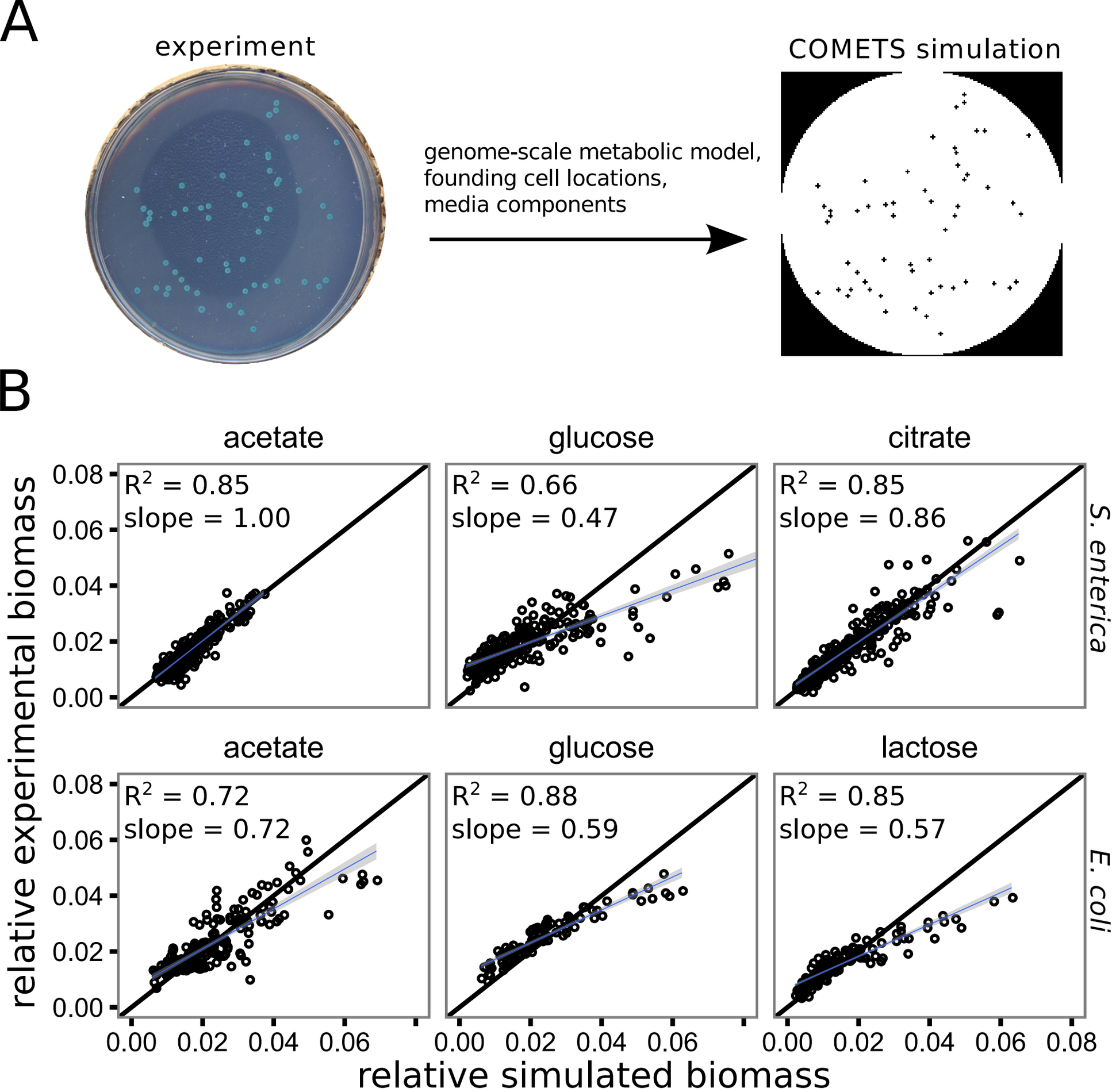
A
experiment
COMETS simulation
genome-scale metabolic model,
founding cell locations,
media components
B
acetate
glucose
citrate
R² = 0.85
slope = 1.00
R² = 0.66
slope = 0.47
R² = 0.85
slope = 0.86
S. enterica
acetate
glucose
lactose
R² = 0.72
slope = 0.72
R² = 0.88
slope = 0.59
R² = 0.85
slope = 0.57
E. coli
relative experimental biomass
relative simulated biomass
0.00
0.02
0.04
0.06
0.08

four metrics to predict spatial effects on colony yield

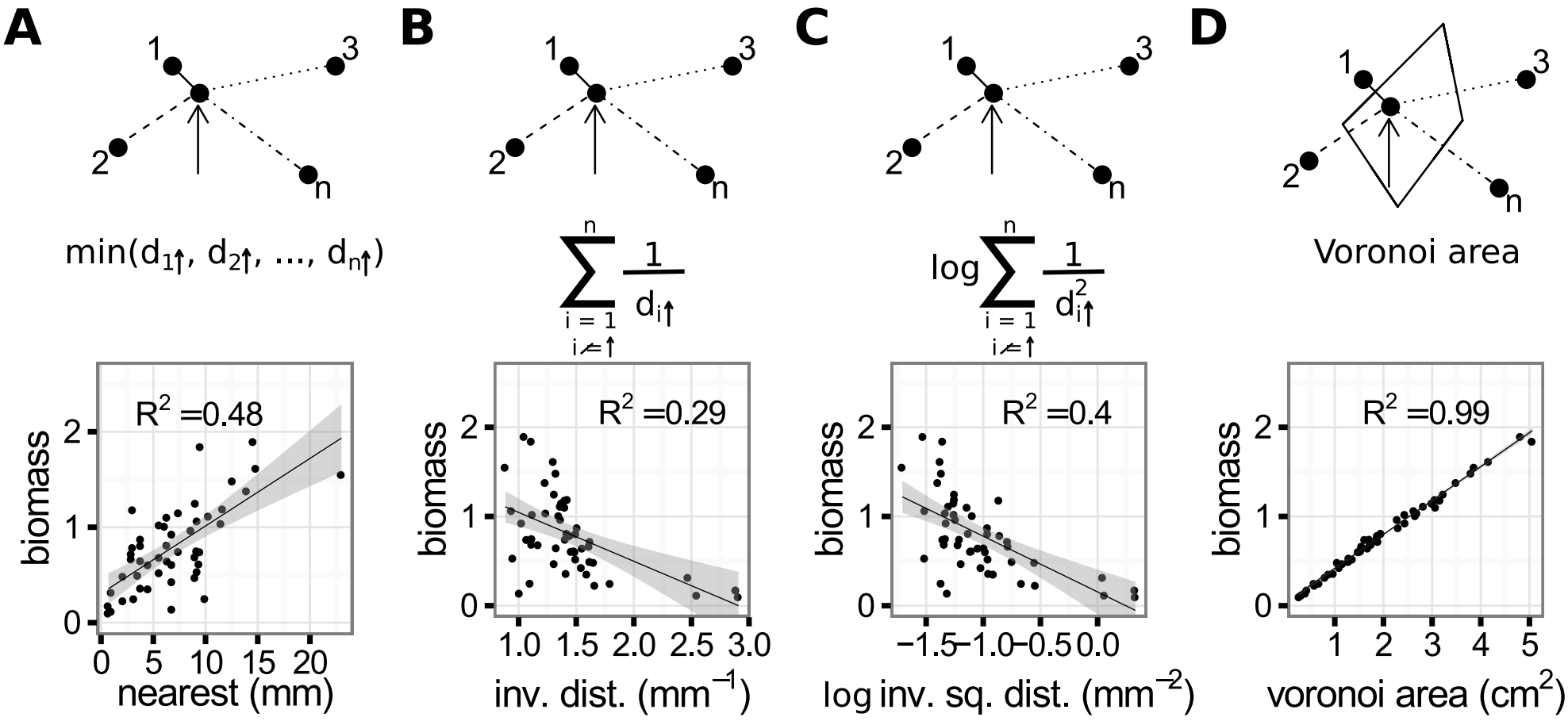

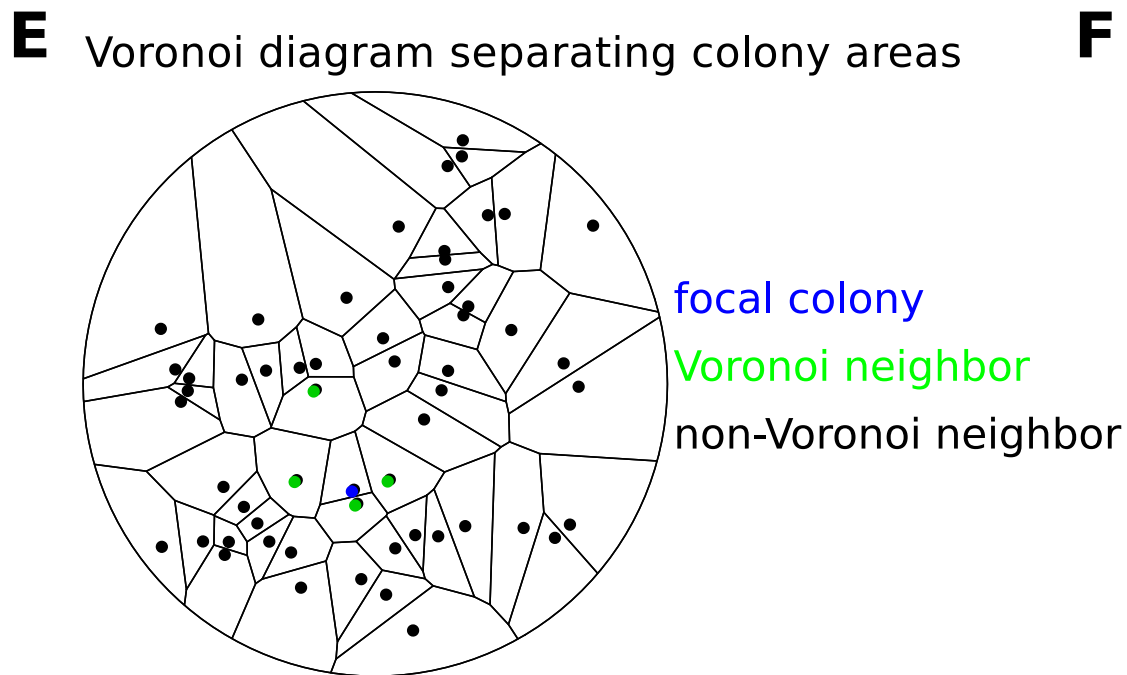

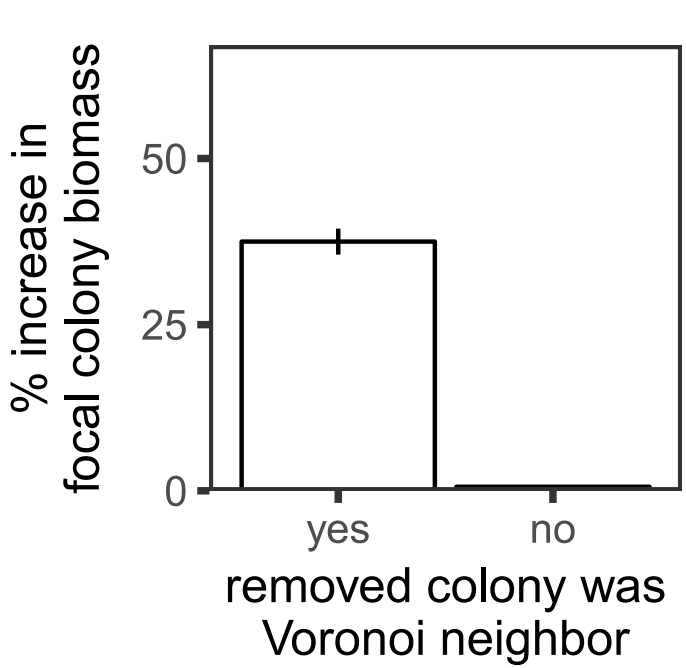

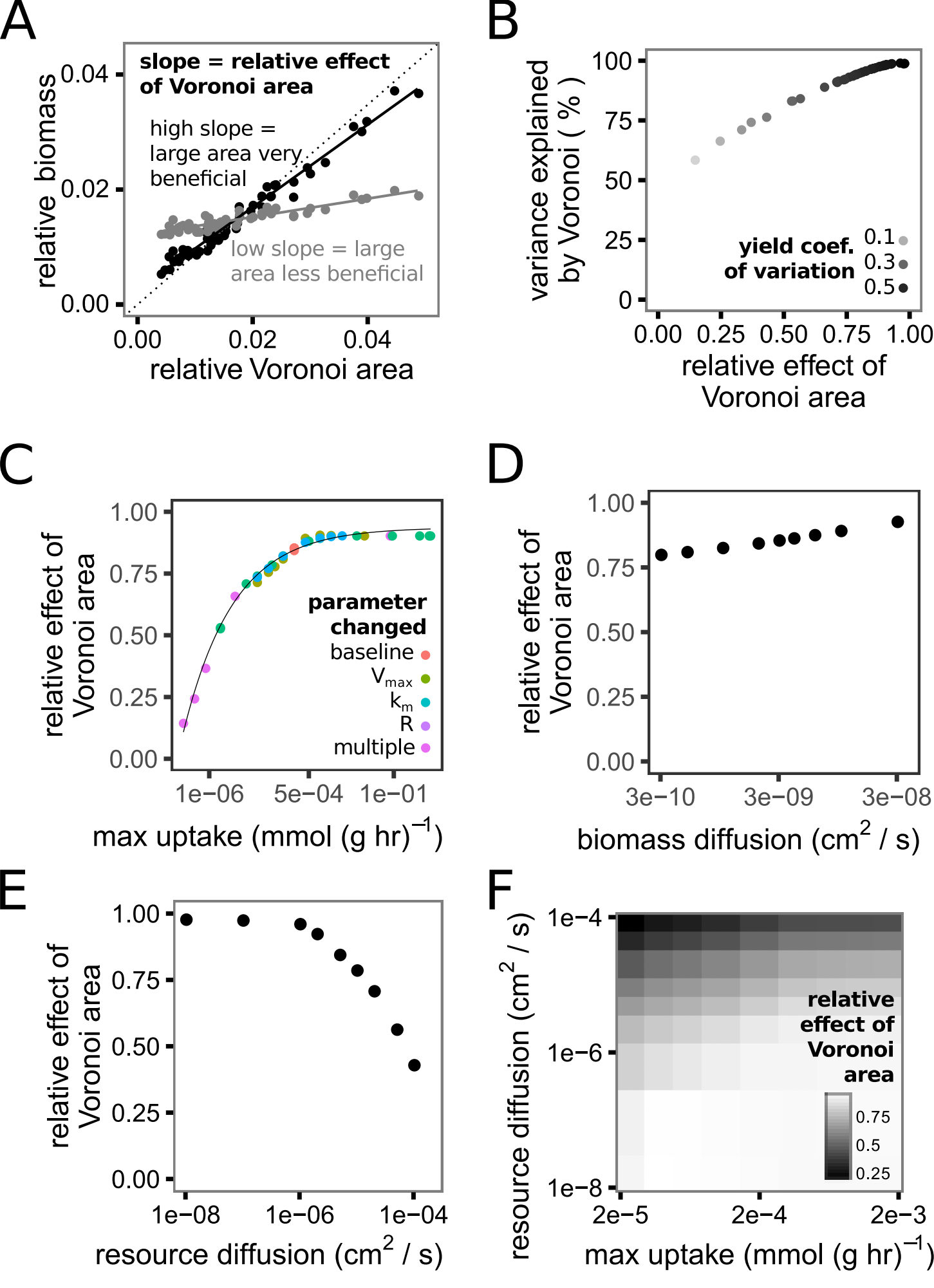
A
slope = relative effect of Voronoi area
high slope = large area very beneficial
low slope = large area less beneficial
relative biomass
0.04
0.02
0.00
0.00
0.02
0.04
relative Voronoi area
B
variance explained by Voronoi (%)
100
75
50
25
0
yield coef. of variation
0.1
0.3
0.5
0.00
0.25
0.50
0.75
1.00
relative effect of Voronoi area
C
relative effect of Voronoi area
1.00
0.75
0.50
0.25
0.00
parameter changed
baseline
V_{max}
k_m
R
multiple
1e−06
5e−04
1e−01
max uptake (mmol (g hr)$^{-1}$)
D
relative effect of Voronoi area
1.00
0.75
0.50
0.25
0.00
3e−10
3e−09
3e−08
biomass diffusion (cm^2 / s)
E
relative effect of Voronoi area
1.00
0.75
0.50
0.25
0.00
1e−08
1e−06
1e−04
resource diffusion (cm^2 / s)
F
resource diffusion (cm^2 / s)
1e−4
1e−6
1e−8
relative effect of Voronoi area
0.75
0.5
0.25
2e−5
2e−4
2e−3
max uptake (mmol (g hr)$^{-1}$)

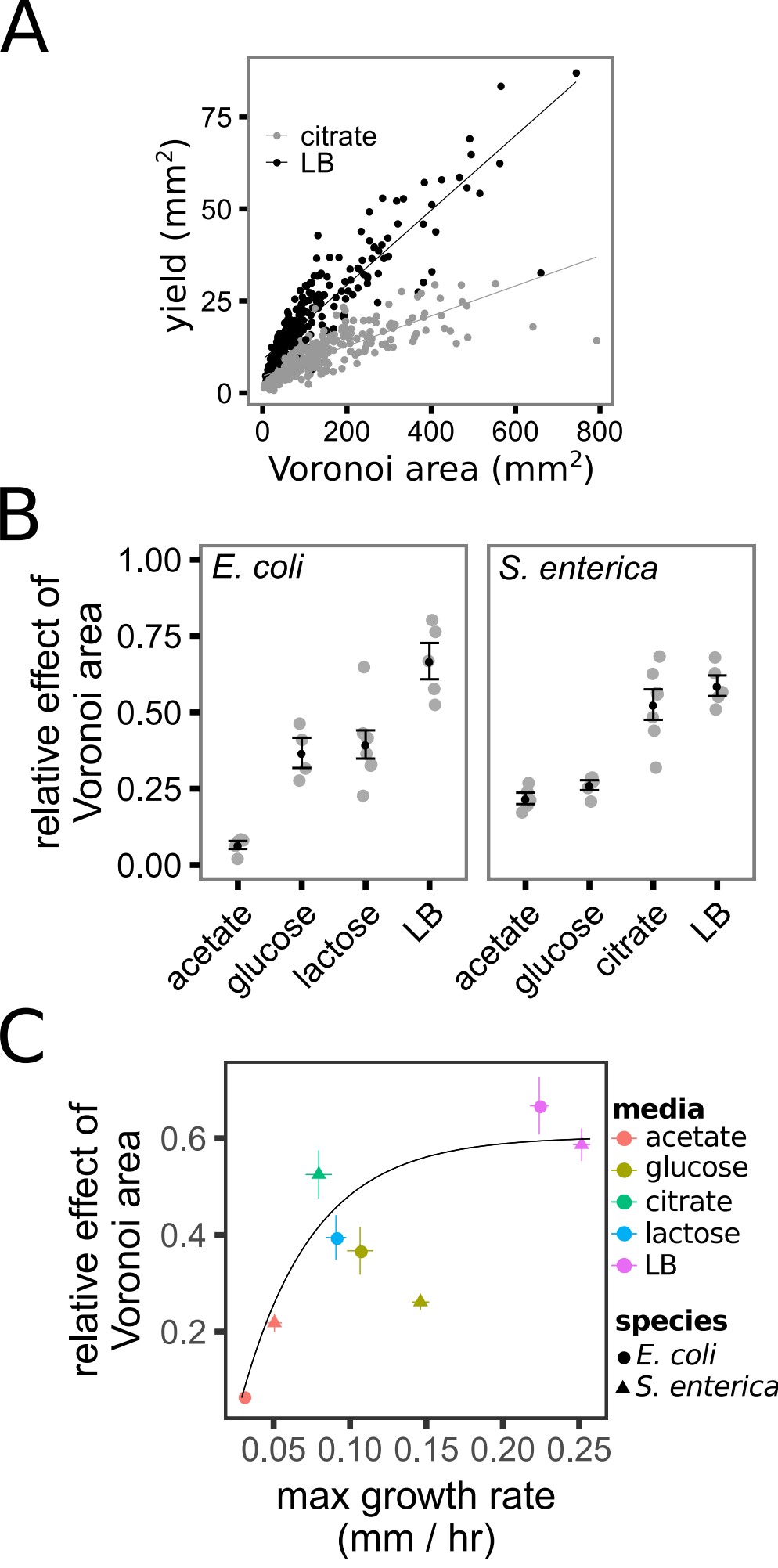
A
citrate
LB
yield (mm²)
Voronoi area (mm²)
B
E. coli
S. enterica
relative effect of Voronoi area
acetate
glucose
lactose
citrate
LB
C
media
acetate
glucose
citrate
lactose
LB
species
E. coli
S. enterica
max growth rate (mm / hr)

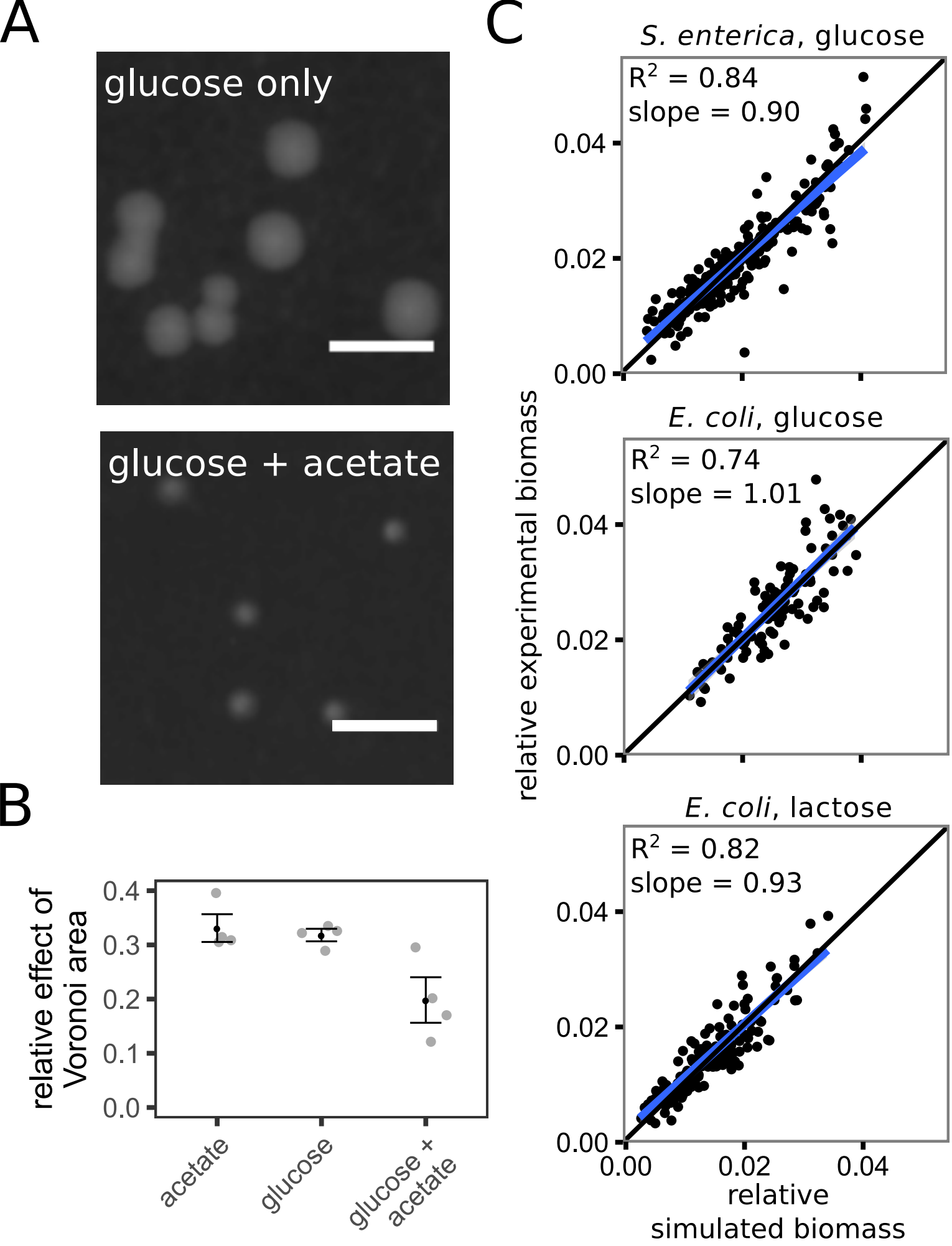
A
glucose only
glucose + acetate
B
relative effect of Voronoi area
0.4
0.3
0.2
0.1
0.0
acetate
glucose
glucose + acetate
C
S. enterica, glucose
R² = 0.84
slope = 0.90
E. coli, glucose
R² = 0.74
slope = 1.01
E. coli, lactose
R² = 0.82
slope = 0.93
relative experimental biomass
0.00
0.02
0.04
relative simulated biomass